

November 14, 1989

## Recent Results and Future Prospects of TOPAZ Experiment

Ichirou Adachi

*Department of Physics, Nagoya University  
Furo-cho, Chikusa-ku, Nagoya 464, Japan*

### ABSTRACT

The TOPAZ detector has accumulated about  $30 \text{ pb}^{-1}$  of data in the energy range,  $\sqrt{s} = 50.0 \sim 61.4 \text{ GeV}$ . We present recent results on (1) search for substructure of leptons, (2) forward-backward asymmetries and total cross sections of  $\mu^+\mu^-$  and  $\tau^+\tau^-$  pair productions, (3) total hadronic cross sections, and (4) search for new particles. Our data are consistent with the Standard Model prediction, except for slightly higher total hadronic cross sections(R-ratio). Considering higher order effects of a heavy top quark mass through the radiative corrections to R-ratios, we obtained an upper bound on top quark mass. Future prospects with high luminosity runs are also discussed.

---

*Talk presented at Workshop on Physics at TeV Scale  
Sep. 28-30, 1989, KEK, Tsukuba, Japan*

## 1. Introduction

We have been conducting experiments for checking validity of the Standard Model and searching for new phenomena beyond the Standard Model. These results have been published[1] and reported[2]. The operation mode of TRISTAN is scheduled to switch from the highest energy runs to high luminosity runs from next year. To maximize physics possibilities at high luminosity TRISTAN, we have added the several detector components into the TOPAZ detector this summer. We have installed small angle calorimeters in the forward region and gap fillers between the barrel and the endcap calorimeters, in order to make the TOPAZ detector hermetic down to 60 mrad. The acceptance for muon tracks are increased from 45° to 25° in polar angle by the installation of forward muon chamber system. A mini-jet chamber as a vertex detector will be installed by the end of this year, which allows us to hunt particle decay vertices. This report presents some new topics and discuss physics possibilities opened up with the upgraded TOPAZ at high luminosity TRISTAN.

## 2. Search for Substructure of Leptons

Substructure of leptons can be studied by searching for deviations from the Standard Model in the differential cross sections for the reactions,  $e^+e^- \rightarrow e^+e^-$ ,  $\mu^+\mu^-$  and  $\tau^+\tau^-$ . The TRISTAN energy region is sensitive to compositeness because relative importance of interference between the Standard Model amplitude and a new interaction term (four fermion contact interaction) is substantial. On the  $Z^0$  pole, on the other hand, the Standard Model amplitude becomes imaginary and can not interfere with the new interaction term. Eichten *et al.* introduced a general form of chiral invariant contact interactions characterized by an energy scale  $\Lambda$ [3]. The effective lagrangian is expressed by:

$$L_{eff} = \frac{g^2}{2\Lambda}(\eta_{LL}J_{LL} + \eta_{RR}J_{RR} + 2\eta_{RL}J_{RL})$$

where  $\Lambda$  is defined as  $g^2/4\pi = 1$  and the largest at  $|\eta_{\alpha\beta}| = 1$  ( $\alpha, \beta = R, L$ ). The following four cases were studied; pure left-handed(LL), pure right-handed(RR), axial-vector( $\Lambda\Lambda$ ) and vector(VV) currents contact interaction corresponding to ( $\eta_{LL} = \pm 1, \eta_{RR} = \eta_{RL} = 0$ ) ( $\eta_{RR} = \pm 1, \eta_{LL} = \eta_{RL} = 0$ ), ( $\eta_{LL} = \eta_{RR} = \eta_{RL} = \pm 1$ ), and ( $\eta_{LL} = \eta_{RR} = \pm 1, \eta_{RL} = \mp 1$ ), respectively.

Fig.1 shows the differential cross sections normalized by the Standard Model predictions and compared with the composite model. The data were corrected for the full radiative correction up to  $O(\alpha^3)$ . No evidence for deviations was observed. 95% C.L. lower limits were calculated and are summarized in Table.1. Our results are comparable with those from PETRA experiments. Note that the relation between integrated luminosity( $L$ ) and sensitive limit of  $\Lambda$  is  $\Lambda \propto (L \cdot s)^{1/4}$ , and that on the  $Z^0$  pole sensitivity to additional four fermi interactions is lost[4]. Accumulating more luminosity, we should be able to improve limits on  $\Lambda$ .

(a)  $e^+e^- \rightarrow e^+e^-$

	LL		RR		VV		AA		$\sqrt{s}$ GeV
	$\Lambda_+$	$\Lambda_-$	$\Lambda_+$	$\Lambda_-$	$\Lambda_+$	$\Lambda_-$	$\Lambda_+$	$\Lambda_-$	
TOPAZ	1.0	1.1	1.2	1.0	2.7	2.5	2.3	1.4	52 ~ 60.8
JADE	1.1	1.4	1.1	1.4	2.5	3.1	2.4	2.3	12 ~ 46.8
PLUTO	1.1	0.76	1.1	0.76	2.2	1.9	2.0	1.6	34.7
TASSO	1.4	3.3	1.4	3.3	3.6	7.1	2.8	2.4	14 ~ 43.6

(b)  $e^+e^- \rightarrow \mu^+\mu^-$

	LL		RR		VV		AA		$\sqrt{s}$ GeV
	$\Lambda_+$	$\Lambda_-$	$\Lambda_+$	$\Lambda_-$	$\Lambda_+$	$\Lambda_-$	$\Lambda_+$	$\Lambda_-$	
TOPAZ	1.5	1.6	1.4	1.5	3.3	2.4	2.0	3.8	52 ~ 60.8
JADE	4.4	2.1	4.4	2.1	5.8	4.8	7.5	2.8	12 ~ 46.8
PLUTO	2.9	0.86	2.9	0.86	2.4	1.6	4.5	1.5	34.7
TASSO	2.3	1.3	2.3	1.3	3.5	1.8	3.2	1.9	35 ~ 46.8

(c)  $e^+e^- \rightarrow \tau^+\tau^-$

	LL		RR		VV		AA		$\sqrt{s}$ GeV
	$\Lambda_+$	$\Lambda_-$	$\Lambda_+$	$\Lambda_-$	$\Lambda_+$	$\Lambda_-$	$\Lambda_+$	$\Lambda_-$	
TOPAZ	0.9	2.2	0.9	2.1	1.6	7.2	2.1	1.6	52 ~ 60.8
JADE	2.2	3.2	2.2	3.2	4.1	5.7	2.7	5.7	12 ~ 46.8

Table.1 A summary of the lower limits on  $\Lambda$  (TeV) at the 95% C.L.

### 3. Forward-Backward Asymmetries and Total Cross Sections of $\mu^+\mu^-$ and $\tau^+\tau^-$ Pair Production

At TRISTAN energies, we have large  $Z^0$  effects in forward-backward asymmetries of lepton pair productions,  $A_{ll}$  ( $\sim -30\%$  for  $l = \mu, \tau$ ), though increase in total cross section,  $R_{ll}$ , is still small ( $\sim 5\%$ ).  $A_{ll}$  has been used to determine the axial vector coupling constants,  $a_\mu$  and  $a_\tau$ . The Standard Model predicts lepton universality, *i.e.* all charged leptons,  $e$ ,  $\mu$  and  $\tau$ , must carry the same axial vector coupling constants.  $R_{ll}$  is sensitive to the vector coupling, although the sensitivity is still statistics-limited. The criteria for  $\mu$  pair events are ; (i) back-to-back charged tracks (acollinearity angle  $\leq 10^\circ$ ) with high momenta coming from the interaction point, (ii) energy deposit in calorimeters being consistent with those of muons, (iii) time of flight measurements consistent with beam associated events. For  $\tau$  pair events, the selection criteria are more complicated because of their weak decays. However, they can be selected by their distinct event topology of 1-1 and 1-3 charged prongs. The obtained asymmetries at each energy point are plotted in Fig.2. To determine the axial vector coupling constants, a global analysis of these asymmetries incorporating PEP/PETRA data was performed assuming  $a_e = -1$ . The resultant values are  $a_\mu = -1.068 \pm 0.054$  and  $a_\tau = -0.858 \pm 0.077$ , which are in good agreement with the  $\mu - \tau$  universality within errors. Assuming lepton universality, we also obtained the universal axial vector coupling constant,  $a_{\mu,\tau} = -0.999 \pm 0.044$ .

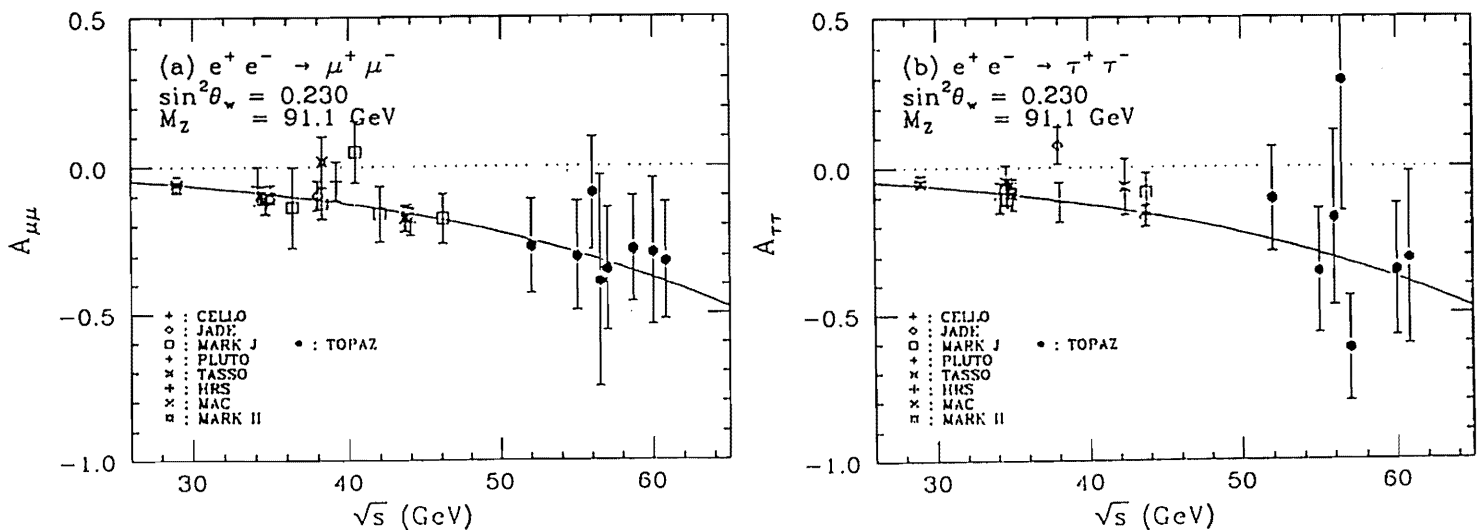


Fig.2 Measured forward-backward asymmetries, (a)  $A_{\mu\mu}$  and (b)  $A_{\tau\tau}$ , as functions of  $\sqrt{s}$ . The solid curve shows the Standard Model prediction for  $M_Z = 91.1 \text{ GeV}/c^2$  and  $\sin^2 \theta_W = 0.23$ .

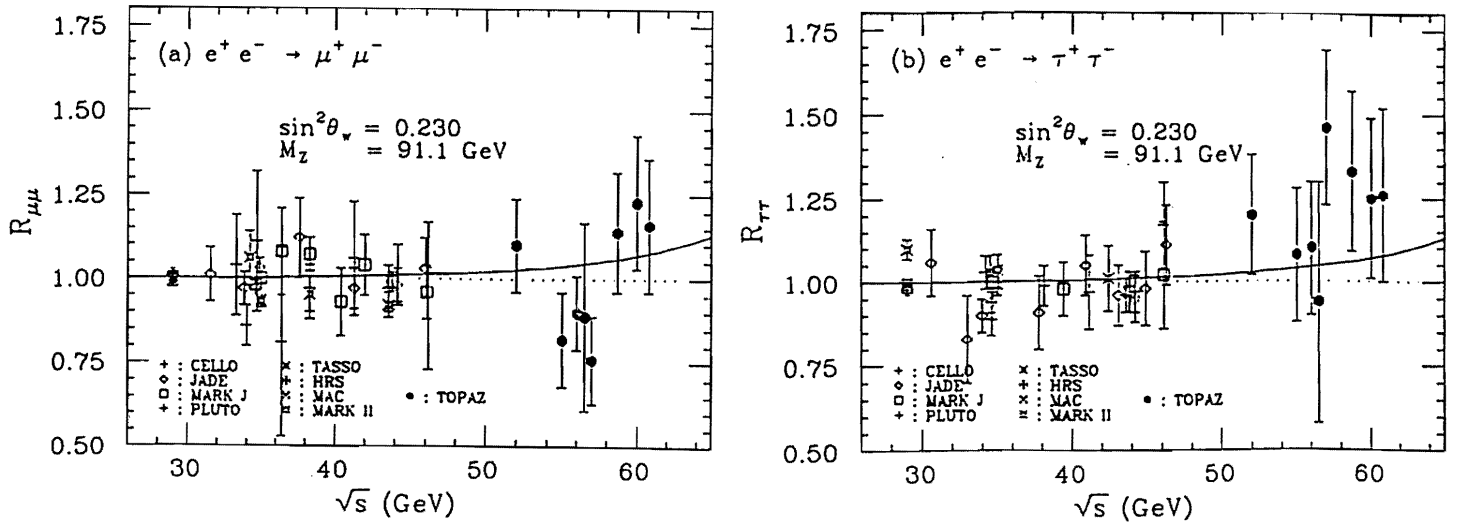


Fig.3 Measured total cross sections, (a) $R_{\mu\mu}$  and (b) $R_{\tau\tau}$ , as functions of  $\sqrt{s}$ . The solid curve shows the Standard Model prediction for  $M_Z = 91.1\text{GeV}/c^2$  and  $\sin^2 \theta_W = 0.23$ .

Total cross sections,  $R_{\mu\mu}$  and  $R_{\tau\tau}$  are shown in Fig.3. As seen in the figure, the present statistics prevents us from ruling out possible deviations from the Standard Model, such as effects of an extra-Z boson. Most of the grand unified theories, *e.g.* the model based on  $E_6$  group, assume new gauge symmetries beyond the Standard Model, which induce extra  $U(1)$ 's after a symmetry breaking, resulting in one or more additional vector bosons[5,6]. Here we consider extra-Z's which appear in the breakdown process;  $E_6 \rightarrow SU(10) \otimes U(1)_\psi \rightarrow SU(5) \otimes U(1)_\chi \otimes U(1)_\psi$ . Assuming that one of the additional  $U(1)$ 's is broken at TeV scale, then the extra-Z,  $Z'$ , is given by the linear combination;  $Z' = Z_\psi \cos \theta_{E_6} + Z_\chi \sin \theta_{E_6}$ . The angles  $\theta_{E_6} = 0, \pi/2, \tan^{-1} \sqrt{3/5}$  and  $\tan^{-1}(-\sqrt{1/15})$  correspond to the  $Z_\psi, Z_\chi, Z_\eta$  and  $Z_\mu$ , respectively. (Detailed discussion can be found in Ref.5.)  $Z'$  and  $Z^0$  are mixed by the following matrix:

$$\begin{pmatrix} Z_1 \\ Z_2 \end{pmatrix} = \begin{pmatrix} \cos \phi & \sin \phi \\ -\sin \phi & \cos \phi \end{pmatrix} \begin{pmatrix} Z^0 \\ Z' \end{pmatrix}$$

where the angle  $\phi$  is given by  $\tan^2 \phi = (M_{Z^0}^2 - M_{Z'}^2)/(M_{Z^0}^2 - M_{Z^0}^2)$ . If such an extra-Z exists, enhancement in  $R_{ll}$  and destructive interference in  $R_{ll}$  could be observed[7]. Fig.4 shows theoretical predictions of  $R_{\mu\mu}$  for various masses of extra-Z. In the same figure, error bars with integrated luminosity of present data and  $200 \text{ pb}^{-1}$  are also plotted. We will be sensitive to  $Z_\psi$  up to  $M_{Z'} \sim 200 \text{ GeV}/c^2$  through measurements of  $R_{\mu\mu}$ .

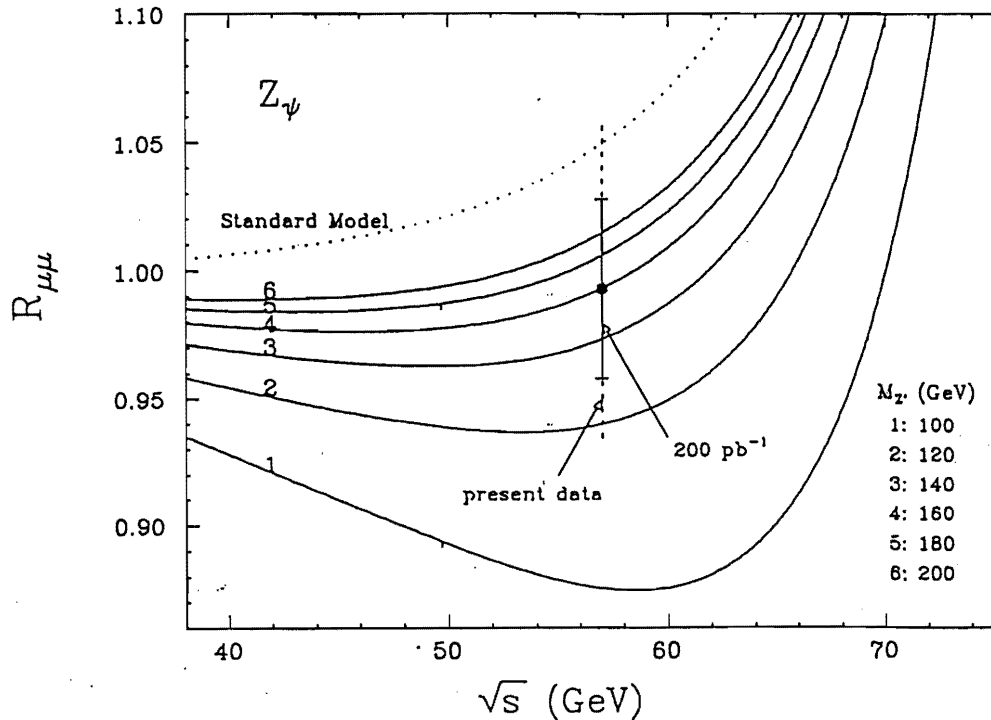


Fig.4  $R_{\mu\mu}$  for  $Z'$  masses from 100 to 200  $\text{GeV}/c^2$  in 10  $\text{GeV}/c^2$  step as a function of  $\sqrt{s}$ . The point with error bar shows data with integrated luminosity of  $30\text{pb}^{-1}$  (present data). Error bars corresponding to  $200\text{pb}^{-1}$  are also shown.  $Z'$  is assumed to be  $\theta_{E_s} = 0(Z_\psi)$ . The dotted curve shows the Standard Model prediction for  $M_Z = 91.1\text{GeV}/c^2$  and  $\sin^2 \theta_W = 0.23$ .

#### 4. Total Hadronic Cross Sections

In the TRISTAN energy region, total hadronic cross section normalized to the QED point-like  $\mu$  pair cross section,  $R$ , increases about 30% due to  $Z^0$  effects, which allows us to determine fundamental parameters in the Standard Model. The contribution from QCD is about 5%, and almost constant.  $R$  is experimentally given by:

$$R = \frac{N_{obs} - N_{BG}}{\epsilon(1 + \delta)L} \cdot \frac{1}{\sigma_{\mu\mu}^0}$$

Where  $N_{obs}$  and  $N_{BG}$  are the number of observed hadronic events and estimated background contamination, respectively.  $\epsilon$  is the detection efficiency, and  $1 + \delta$  is the radiative correction factor.  $L$  is the integrated luminosity, and  $\sigma_{\mu\mu}^0$  is the lowest order point-like QED cross section of  $\mu$  pair production. Hadronic events are selected by; (i) the number of "good" charged tracks in TPC  $\geq 5$ , (ii) visible energy ( $E_{vis}$ )  $\geq$  the beam energy ( $E_{beam}$ ), (iii) momentum balance in the beam direction  $\leq 0.4 \cdot E_{vis}$ , (iv) invariant jet mass  $\geq 2.5 \text{ GeV}/c^2$ , and (v) the number of clusters having energy greater than  $E_{beam}/2 \leq 1$ . The obtained number of hadronic events is 3462 in total. In calculating the

radiative correction factor,  $1 + \delta$ , we used a new program developed by J. Fujimoto and Y. Shimizu[8], instead of the traditional Berends, Kleiss and Jadach(BKJ) method[9]. This new method contains all radiative processes in electroweak theory up to  $O(\alpha^3)$ , and is called hereafter “full electroweak radiative correction”. The difference between the full electroweak radiative correction and the BKJ is about 3% at  $\sqrt{s} = 60$  GeV, as shown Fig.5-(a). Here we chose the following values as input;  $M_Z = 91.9$  GeV/c<sup>2</sup>[10],  $M_{top} = 40$  GeV/c<sup>2</sup> and  $M_{Higgs} = 100$  GeV/c<sup>2</sup>. The dependence of  $1 + \delta$  on these input values are shown in Fig.5(b)-(d). These deviations were included in systematic uncertainty. Systematic errors were estimated to be 4.0% for luminosity measurement, 3.3% for acceptance and 1.9% for radiative corrections.

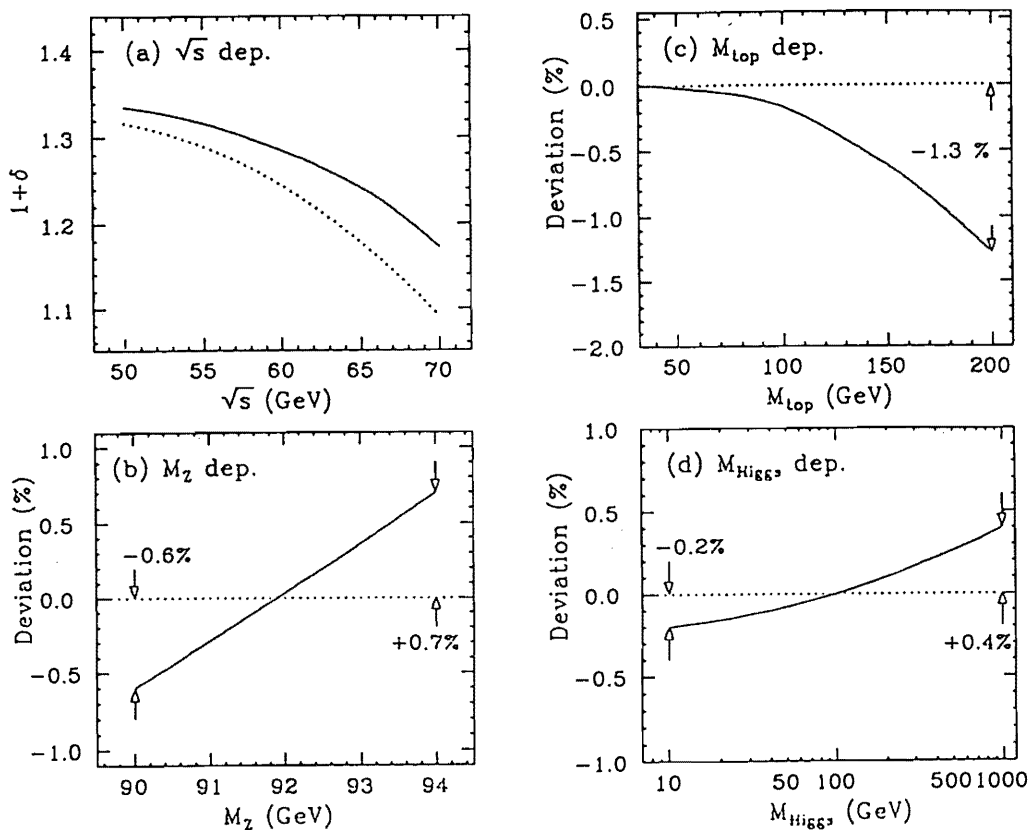


Fig.5 (a)The full electroweak radiative correction factor,  $1 + \delta$ , as a function of  $\sqrt{s}$  for the standard constants of  $M_Z = 91.9$  GeV/c<sup>2</sup>,  $M_{top} = 40$  GeV/c<sup>2</sup>,  $M_{Higgs} = 100$  GeV/c<sup>2</sup> and  $k_{max} = 0.99$ . The BKJ correction is also shown as a dotted curve. They are significantly different in the TRISTAN energy region. (b)The dependence of  $1 + \delta$  on  $M_Z$ , where the vertical scale is the deviation of  $1 + \delta$  from the value calculated using the standard constants at  $\sqrt{s} = 60$  GeV. (c)The same as (b) but shows the dependence on  $M_{top}$  and (d)on  $M_{Higgs}$ .

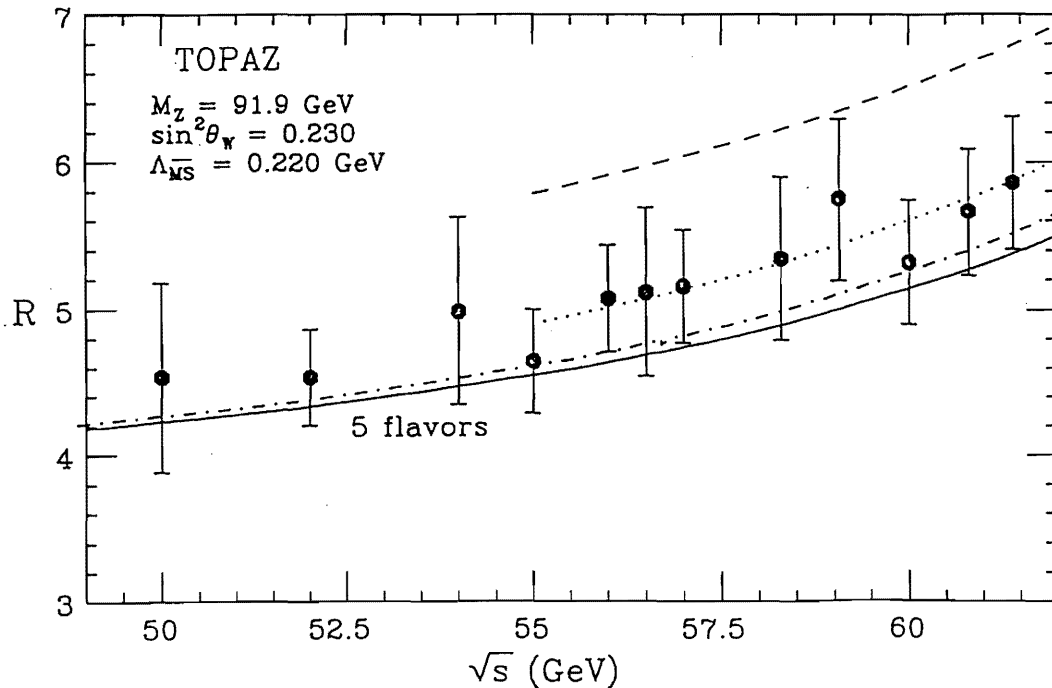


Fig.6 The resultant R values. The error bars include the statistical and systematic errors added in quadrature. The solid curve shows the Standard Model prediction with  $M_Z = 91.9 \text{ GeV}/c^2$ ,  $\sin^2 \theta_W = 0.230$  and  $\Lambda_{\overline{MS}} = 0.327 \text{ GeV}$ . The dashed and dotted curves show the R values expected for open production of top and  $b'$  quarks, respectively. The dot-dashed curve is for  $M_Z = 91.1 \text{ GeV}/c^2$ ,  $\sin^2 \theta_W = 0.230$  and  $\Lambda_{\overline{MS}} = 0.3 \text{ GeV}$ .

The obtained R values are plotted in Fig.6. Our data show no open top production, but are systematically “higher” than the Standard Model prediction with  $M_Z = 91.9 \text{ GeV}/c^2$  above  $\sqrt{s} = 56 \text{ GeV}$ . Some possibilities for the “higher” R values have been discussed and checked. One such possibility is heavy flavor productions, which have been excluded by various analyses such as shape analysis, isolated muon search and isolated photon search[2,11]. Another possibility is a lower  $M_Z$ , as low as  $88 \text{ GeV}/c^2$ [12], but  $M_Z$  has been determined precisely to be  $91.11 \pm 0.23 \text{ GeV}/c^2$  and  $90.9 \pm 0.3(\text{stat} + \text{sys}) \pm 0.2(\text{scale}) \text{ GeV}/c^2$  at Mark II/SLC[13] and CDF/Tevatron[14], respectively. Here we consider a higher order effect of  $M_{top}$  through the radiative corrections. As seen in Fig.5-(c), a larger  $M_{top}$  gives smaller  $1 + \delta$ , making our R values higher. For the purpose of this study, we fixed  $M_Z$  to be  $91.1 \text{ GeV}/c^2$  and took  $M_{top}$  and  $\Lambda_{\overline{MS}}$  as free parameters.



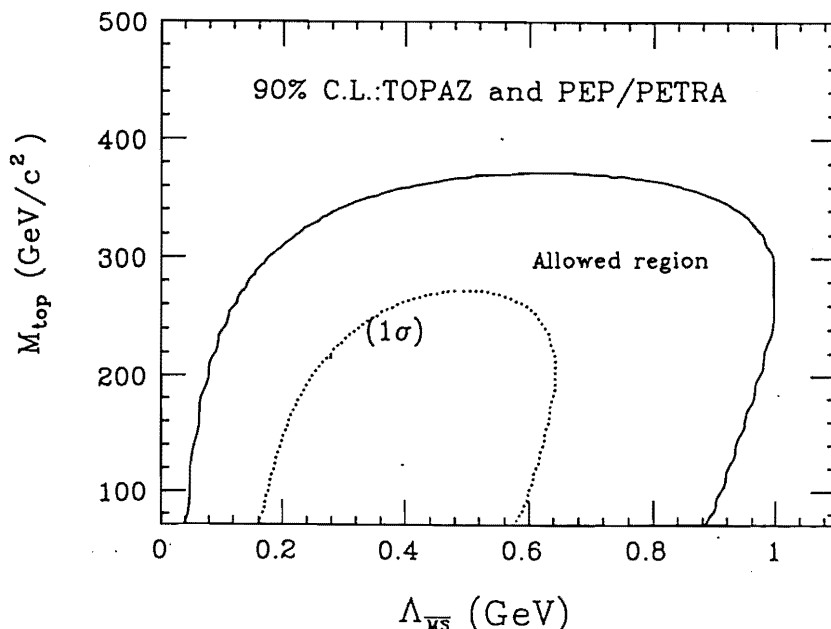


Fig.7 Region allowed at the 90% C.L. in the plane of  $M_{top}$  and  $\Lambda_{\overline{MS}}$  for  $M_{Higgs} = 100 \text{ GeV}/c^2$ . The  $1\sigma$  contour is drawn as a dotted curve.

In this analysis,  $\sin^2 \theta_W$  was calculated by the formula:

$$\sin^2 \theta_W = \frac{1}{2} \left( 1 - \sqrt{1 - \frac{4\pi\alpha}{\sqrt{2}G_F M_Z^2 (1 - \Delta r)}} \right)$$

with  $\Delta r$  as a function of  $M_{top}$ [15], and  $1 + \delta$  was parametrized as the convolution of the 4-th and 2-nd order polynomial equations of  $M_{top}$  and  $\sqrt{s}$ , respectively. In this way, the heavy top quark can alter significantly both our R values through the radiative correction factor and theoretical values through the value of  $\sin^2 \theta_W$ . A global fit to our R values together with PEP/PETRA results was carried out in a consistent way, described above, by the CELLO method[16]. The obtained results are shown in Fig.7 as a contour plot of  $M_{top}$  and  $\Lambda_{\overline{MS}}$  at the 90% C.L., where the  $1\sigma$  contour was also drawn. This fit with  $M_{top} \sim 100 \text{ GeV}/c^2$  gives better agreement with our "high" R values than that with  $M_{top} = 40 \text{ GeV}/c^2$ , which could be explanation of "high" R values. Because this fit becomes poor if  $M_{top}$  goes heavier, we obtained an upper bound,  $M_{top} < 366 \text{ GeV}/c^2$ , at the 90% C.L. for  $M_{Higgs} = 100 \text{ GeV}/c^2$ . A more stringent limit of  $M_{top} < 180 \text{ GeV}/c^2$  (90% C.L.,  $M_{Higgs} = 100 \text{ GeV}/c^2$ ) has been given by U. Amaldi *et al.*[17]. However, the determination of  $M_{top}$  from only R values is important to test the electroweak radiative corrections of the Standard Model. The best fit value of  $\Lambda_{\overline{MS}}$  is  $0.354^{+0.289}_{-0.194} \text{ GeV}$ , which is consistent with the other measurements[18].

## 5. Search for New Particles

Here we make a short comment on new particle search. New particles within the Standard Model and beyond the Standard Model have been searched for, and the results are summarized in Table.2 in the form of mass limits at the 95% C.L. Some of mass limits listed here have been already extended by Mark II/SLC[19]. Do we have no chance of new particle search ? Fig.8 shows the total cross section for  $e^+e^- \rightarrow \gamma \tilde{\gamma}\tilde{\gamma}$  together with that for  $e^+e^- \rightarrow \gamma\nu\bar{\nu}$ . TRISTAN is the best place for  $\tilde{\gamma}$  search by detecting single photon final state. On the contrary,  $Z^0$  pole experiments should suffer from large  $\gamma\nu\bar{\nu}$  background. Needless to say, a hermetic calorimetry is crucial for single photon experiment, which has been satisfied by the upgrade in this summer. If we accumulate integrated luminosity of  $100 \text{ pb}^{-1}$  and find no excess, it will be possible to extend the  $m_{\tilde{\gamma}}$  limit over that of the ASP experiment[20] which is the best so far.

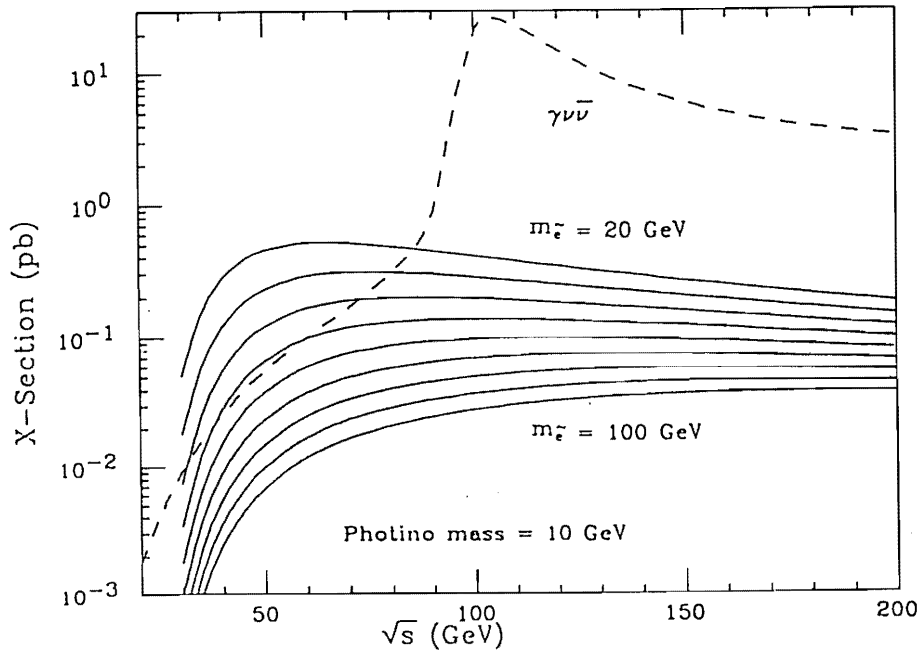


Fig.8  $\gamma \tilde{\gamma}\tilde{\gamma}$  cross sections integrated over the acceptance of the upgraded TOPAZ detector for selectron masses  $m_{\tilde{e}}$  from 20 to 100  $\text{GeV}/c^2$  in 10  $\text{GeV}/c^2$  step as functions of  $\sqrt{s}$ . The dashed curve is for  $\gamma\nu\bar{\nu}$ .

Model	Particle	Search Method	95% CL Lower Mass Limit
Standard	t	Isolated $\mu$	29.9 GeV
	$b'$	Isolated $\mu$	28.4 (CC)
		Isolated $\gamma$	28.3 (FCNC)
		Back-to-back 4jet	
$L^\pm$	Acoplanar jets	29.9	
SUSY <sup>(*1)</sup>	$\tilde{e}$	Acoplanar $e^+e^-$	29.0 ( $m_L = m_R$ ) 28.1 ( $m_L \gg m_R$ )
	$\tilde{\mu}$	Acoplanar $\mu^+\mu^-$	25.8 ( $m_L = m_R$ ) 24.0 ( $m_L \gg m_R$ )
	$\tilde{\tau}$	Acoplanar $\tau^+\tau^-$	24.2 ( $m_L = m_R$ ) 21.3 ( $m_L \gg m_R$ )
	$\tilde{q}(2/3)$	Acoplanar Jets	26.3 ( $m_L = m_R$ ) 24.4 ( $m_L \gg m_R$ )
	$\tilde{\chi}$	Acoplanar $e^+e^-$ , $\mu^+\mu^-$ , $\tau^+\tau^-$ , Jets	26.8 <sup>(*2)</sup> 27.7 <sup>(*3)</sup>
Composite <sup>(*4)</sup>	$e^*$	$e^+e^-\gamma\gamma$	29.7
	$\mu^*$	$\mu^+\mu^-\gamma\gamma$	28.3
	$\tau^*$	$\tau^+\tau^-\gamma\gamma$	27.6
Any Model with Stable Heavy Charged Particle	Q=2/3	Pair of Abnormal dE/dX	24.6
	J=0 Q=1		25.6
	Q=4/3		26.6
	Q=2/3	Tracks	29.2
	J=1/2 Q=1		28.2
Q=4/3		25.7	
Stable scalar quark	Q=2/3	Any tracks with Abnormal dE/dX	24( $m_L = m_R$ ) 13( $m_L \gg m_R$ )
	Q=1/3		12( $m_L = m_R$ ) 10( $m_L \gg m_R$ )

- (\*1) LSP =  $\tilde{\gamma}$ ,  $m_{\tilde{\gamma}} = 0$ , Target Particle = NLSP  
(\*2) Limits are independent of decay branching ratios.  
(\*3) Limits assuming equal leptonic branching ratios.  
(\*4) Pointlike coupling

Table.2 A summary of the results from new particle searches.

## 6. Summary

- 1 . Compositeness of  $e, \mu$  and  $\tau$  was tested and lower limits on  $\Lambda$  were calculated to be  $\sim 2$  TeV at the 95% C.L.
- 2 . Measured asymmetries and cross section sections were consistent with the Standard Model prediction, and the universality between  $\mu$  and  $\tau$  is still valid.
- 3 . Our R values above  $\sqrt{s} = 56$  GeV is systematically “high”. In the framework of the Standard Model, a global fit to our “high” R values together with PEP/PETRA results seems to be in favor of a heavy top quark mass, about 100 GeV/ $c^2$ .
- 4 . New particles have been searched for and no excess was found.

Accumulating more luminosity with the upgraded TOPAZ detector, we will be able to test the Standard Model more precisely and also be able to search for new physics, *e.g.* extra-Z via  $\mu$  pair production and  $\tilde{\gamma}$  via single photon experiment. Especially, it will be possible to search for a source of our “high” R values.

## REFERENCES

1. TOPAZ Collab., I. Adachi *et al.*, *Phys. Lett.* **200B**(1988)391, *Phys. Rev. Lett.* **60**(1988)97, *Phys. Rev.* **D37**(1988)1339, *Phys. Lett.* **208B**(1988)319, *Phys. Lett.* **218B**(1989)105, *Phys. Lett.* **227B**(1989)495, *Phys. Lett.* **228B**(1989)553.
2. TOPAZ Collab., S. Suzuki, Proc. of the KEK Topical Conference on  $e^+e^-$  Collision, May, 1989, KEK, Japan, DPNU-89-32.
3. E. Eichten, K. D. Lane and M. E. Peskin, *Phys. Rev. Lett.* **50**(1983)811.
4. F. Schrempp, DESY 89-047.
5. D. London and J. L. Rosner, *Phys. Rev.* **D34**(1986)1530 and references quoted therein.
6. K. Hagiwara, R. Najima, M. Sakuda and N. Terunuma, KEK preprint 89-57
7. A. A. Pankov and I. S. Satsunkevich, *Sov. J. Nucl. Phys* **47**(5)849, May, 1988.
8. J. Fujimoto and Y. Shimizu, *Mod. Phys. Lett.* **A3**(1988)581;  
J. Fujimoto, Ph.D. Thesis, Nagoya University, 1987.
9. F. A. Berends and R. Kleiss, *Nucl. Phys.* **B178**(1981)141;  
F. A. Berends, R. Kleiss and S. Jadach, *Nucl. Phys.* **B202**(1982)63.
10. Particle Data Group, *Phys. Lett.* **204B**(1988)1.
11. TOPAZ Collab., contributed paper for the XIV International Symposium on Lepton and Photon Interactions, to be published.
12. T. Nozaki, Proc. of the XXIX Recontres Moriond, March, 1989, Les Arcs, France, KEK preprint 89-19;  
TOPAZ Collab., contributed paper for the XIV International Symposium on Lepton and Photon Interactions.
13. Mark II Collab., G. S. Abrams *et al.*, *Phys. Rev. Lett.* **63**(1989)724.
14. CDF Collab., F. Abe, *et al.*, *Phys. Rev. Lett.* **63**(1989)720.
15. W. J. Marciano and A. Sirlin, *Phys. Rev.* **D29**(1984)945;  
Z. Hlilki, *Prog. Theor. Phys.* **68**(1982)2134, *Prog. Theor. Phys.* **71**(1984)663.
16. CELLO Collab., H. J. Berend *et al.*, *Phys. Lett.* **113B**(1987)400.
17. U. Amaldi *et al.*, *Phys. Rev.* **D36**(1987)1385.

18. T. Kamae, Proc. of the XXIV International Conference on High Energy Physics, Aug, 1988, Munich, Germany, UT-HE-88/05.
19. Mark II Collab., A. Weinstein, Talk at the XIV International Symposium on Lepton and Photon Interactions, Aug, 1989, Stanford, U.S.A.
20. ASP Collab., C. Hearty *et al.*, *Phys. Rev. Lett.* **58**(1987)1711, *Phys. Rev.* **D39**(1989)3207.